Optical Properties and Band Structure of Trigonal Selenium

SIMPEI TUTIHASI AND INAN CHEN
Research Laboratories, Xerox Corporation, Rochester, New York
(Received 9 February 1967)

The reflectivity spectra of single crystals of trigonal selenium have been measured at 300 and 20°K between 1.0 and 5.9 eV for light polarized in directions parallel and perpendicular to the c axis. The Kramers-Kronig relation has been applied to obtain the wavelength dependence of the optical constants. At 20°K, the imaginary part of the dielectric constant for perpendicular polarization shows one sharp peak at 1.95 eV which has been interpreted as being due to exciton absorption. Another sharp peak in the parallel polarization spectrum at 3.09 eV has also been attributed to an exciton absorption. All other observed peaks have been interpreted in terms of transitions at symmetry points in k space. Based on the double-group selection rule and the observed transition energies, a band structure for trigonal selenium is proposed and is compared with published theoretical calculations.

I. INTRODUCTION

THE purpose of the work reported in this paper was to investigate the optical properties of trigonal Se single crystals in the fundamental absorption region at low temperatures and to compare the data with existing theoretical calculations in an attempt to understand the band structure of the material. The absorption coefficient of the crystal reaches above 10^5 cm^{-1} in the fundamental absorption region, and the preparation of thin crystalline samples for direct transmission measurements is extremely tedious. In the present work the optical constants are determined by a Kramers-Kronig analysis[1–3] of normal-incidence reflectance spectra. This process evaluates the real and imaginary parts of the dielectric constants ϵ_1 and ϵ_2 which describe the optical properties of the crystal.

The structure of trigonal Se consists of helical chains with their axes parallel to the c axis. The atoms along the chain are held together by strong covalent bonds while the forces between atoms of adjacent chains are of the weak van der Waals type. A band-structure study for a helical Se chain was carried out by Reitz.[4] He employed a tight-binding approximation in which only the nearest-neighbor interactions were considered, and the chains were assumed to be completely independent of each other. More recently, Olechna and Knox[5] made Reitz's calculation quantitative, using Hartree-Fock wave functions and also including s-p mixing. They were thus able to explain the reflectivity data reported by Stuke and Keller,[6] whose measurements have so far been the most detailed and extensive. Sandrock and Treusch[7] took a different approach to the problem, calculating the band structure of trigonal Se crystals by the Kohn-Rostoker method.[8] Their results indicate a direct band-gap at the Brillouin-zone corner H (Fig. 1); according to Olechna and Knox[5] the band gap in single Se chains is located at Z.

In spite of this recent progress in the theoretical studies, experimental knowledge of the band structure of trigonal Se is limited mainly because of the lack of optical data on the material in its fundamental absorption region. The reflectivity spectra of single crystals of trigonal Se were reported by Prosser,[9] Gobrecht and Tausend,[10] and more recently by Stuke and Keller.[6] Their measurements were made at room temperature and, because of thermal broadening, showed only gross structure. In addition, their investigations did not cover the spectral region above 4.1 eV, thus making the application of a Kramers-Kronig analysis difficult.

We have measured the reflectivity spectra of single crystals of trigonal Se at 20°K, as well as at 300°K, and have found considerable fine structure. At 20°K, the spectra developed a number of peaks including two peaks attributed by us to excitons,[11] which are not observed at room temperature. We found it difficult to assign the observed peaks using the available band-structure models.[5,7] Therefore, we have carried out a group-theoretical study of the electronic energy levels of trigonal Se, including the effect of spin-orbit coupling. Combining the information obtained from this analysis

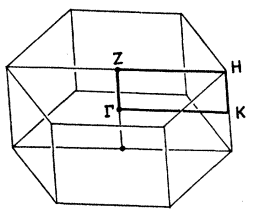

FIG. 1. Brilluoin zone for the lattice of trigonal Se.

[1] F. C. Jahoda, Phys. Rev. **107**, 1261 (1957).
[2] H. R. Philipp and E. A. Taft, Phys. Rev. **113**, 1002 (1959); **120**, 37 (1960); **127**, 159 (1962).
[3] H. R. Philipp and H. Ehrenreich, Phys. Rev. **129**, 1550 (1963); **131**, 2016 (1963).
[4] J. R. Reitz, Phys. Rev. **105**, 1233 (1956).
[5] D. J. Olechna and R. S. Knox, Phys. Rev. **140**, A986 (1965).
[6] J. Stuke and H. Keller, Phys. Status Solidi **7**, 189 (1964).
[7] R. Sandrock, dissertation, Marburg University, Lahn, Germany, 1965 (unpublished); R. Sandrock and J. Treusch, Solid State Commun. **3**, 361 (1965); Phys. Status Solidi **16**, 487 (1966).
[8] W. Kohn and N. Rostoker, Phys. Rev. **94**, 1111 (1954).
[9] V. Prosser, Czech. J. Phys. **B10**, 306 (1960); in *Proceedings of the International Conference on Semiconductor Physics, 1960* (Academic Press Inc., New York, 1961), p. 993.
[10] H. Gobrecht and A. Tausend, Z. Physik **161**, 205 (1961).
[11] S. Tutihasi and I. Chen, Solid State Commun. (to be published).

and the experimental results we have proposed a band structure for trigonal Se.

II. EXPERIMENTAL

Experiments were carried out on single crystals of trigonal Se. The single crystals were grown from melts,[12] and were cylindrical with a diameter of about 8 mm. Crystals were cleaved along the $(10\bar{1}0)$ plane; the cleaved surfaces were etched with CrO_3 dissolved in concentrated hydrochloric acid to obtain mirror quality. The crystals thus prepared for measurements had dimensions of approximately 8 mm×8 mm×2 mm, with two parallel flat surfaces. To minimize the problem of reflection from the rear surface in the long-wavelength region, the back surfaces of the crystals were made rough by rubbing with carborundum powder.

Because trigonal Se is uniaxial, reflectance measurements were made with light polarized in directions parallel ($E\|c$), and perpendicular ($E\perp c$), to the c axis on the $(10\bar{1}0)$ surface at approximately 5° angle of incidence in the spectral range between 1.0 and 5.9 eV. A Leiss, double monochromator was used with a pair of silica prisms for the 2.5- to 5.9-eV region and with a pair of flint glass prisms for the 1.0- to 2.5-eV region. The resolution of the instrument was estimated to be better than 0.01 eV throughout the spectral range. A Glan-type polarizer which transmits from 0.54 to 6.2 eV provided polarized beams.

The optical arrangement is shown schematically in Fig. 2. The liquid-helium reservoir of the cryostat in Fig. 2 is rotatable around its axis. A sample crystal and an Al reference mirror are mounted on the sample holder F, which is attached to the bottom of the reservoir. By rotating the reservoir, the crystal or the Al reference mirror can be brought into the light beam for measurements.

The signal output from the photomultiplier [EMI-9558Q for the uv and visible regions; EMI-9684 for the infrared region] was recorded continuously while the monochromator was driven mechanically. The results obtained were then corrected for the reflectivity of the Al reference mirror.

Possible contamination of the sample surface by the condensation of residual gases in the cryostat at low temperatures was checked by measuring the reflectivity at various time intervals after the crystal was cooled. The contamination was found to be too small to influence the measurements. By repeated measurements on four different crystal samples, the uncertainty in the value of the reflectance data was estimated to be within 5%.

The reflectivity spectra thus obtained are shown in Fig. 3; the broken-line curves were measured at 300°K

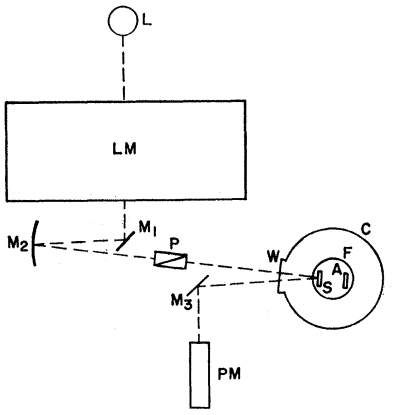

LEGEND:
L : LIGHT SOURCE
LM : LEISS DOUBLE PRISM MONOCHROMATOR
M_1,M_3 : PLANE MIRRORS
M_2 : SPHERICAL MIRROR
P : GLAN TYPE POLARIZER
PM : PHOTOMULTIPLIER
C : CRYOSTAT
W : SILICA WINDOW
F : SAMPLE HOLDER
S : SAMPLE CRYSTAL
A : REFERENCE Al MIRROR

FIG. 2. Schematic diagram of the experimental apparatus. The window W is tilted about 10° downward to prevent the beam reflected by the window from reaching the detector.

and the solid-line curves at 20°K. The room-temperature spectra are similar to those reported by Stuke and Keller.[6] The first sharp peak observed at 1.94 eV for $E\perp c$ at 20°K has been interpreted as being due to direct exciton absorption, a detailed account of which has been published elsewhere.[11]

Now, in order to execute a Kramers-Kronig analysis of the reflectivity spectra shown in Fig. 3, it is necessary to have some knowledge of the reflectivity[1] beyond 5.9

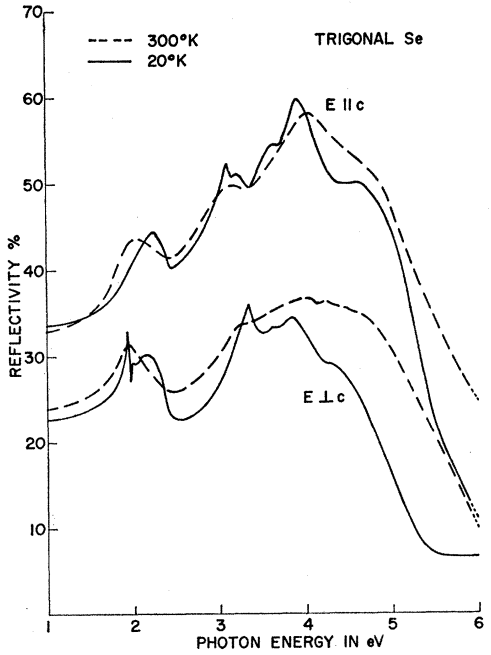

FIG. 3. Reflectivity spectra of trigonal Se.

[12] R. C. Keezer and J. W. Moody, Appl. Phys. Letters 8, 233 (1966); R. C. Keezer, C. Wood, and J. W. Moody, in Proceedings of an International Conference on Crystal Growth, Boston, 1966, p. 119 (to be published in J. Phys. Chem. Solids Suppl.).

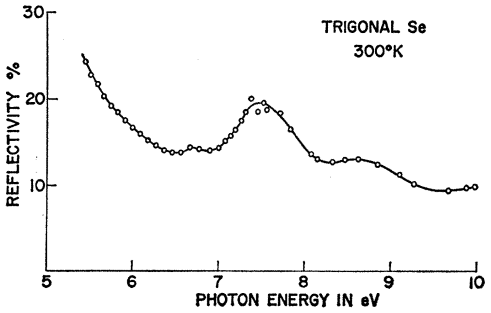

FIG. 4. Reflectivity spectrum of trigonal Se in vacuum uv region at 300°K.

eV. This would enable us to approximate the end segments of the spectra to the frequency region reasonably remote from that of interest (1.6 to 5.5 eV). Figure 4 shows the reflectivity spectrum of trigonal Se crystals measured at 300°K with unpolarized light on the $(10\bar{1}0)$ surface at 15° angle of incidence. The data for Fig. 4 were obtained using a Tropel vacuum uv monochromator with a Smith reflectometer attachment.[13] The resolution in this region was approximately 0.05 eV.

In the actual computation of the Kramers-Kronig integrals, the end segment (5.9 to 10.0 eV) of each reflectivity spectrum was assumed to decrease exponentially. This approximation is justified because the contributions to the integrals from symmetric portions of the remote spectrum tend to cancel each other,[1] and in this region, the reflectivity (Fig. 4) shows no significant structure. The slope of the high-energy end segment was adjusted numerically so that the lower-energy edge of the absorption spectra decreased exponentially and reached a value[10] less than 10^2 cm^{-1} below 1.5 eV.

Figures 5 to 8 show the real and imaginary parts of the dielectric constant ϵ_1 and ϵ_2, respectively, evaluated from the spectra shown in Fig. 3. Approximately 180

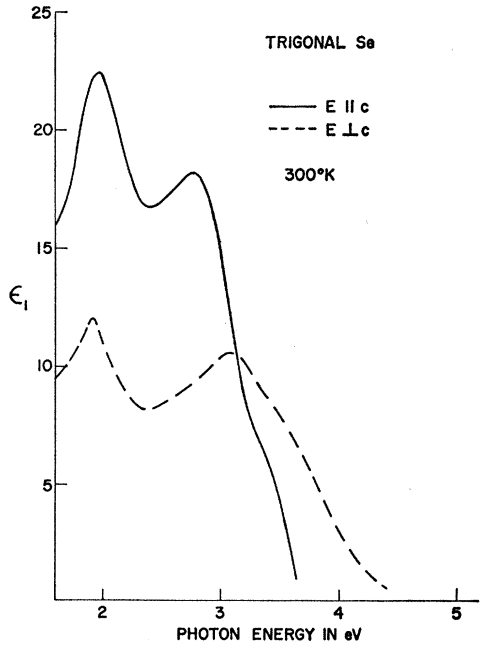

FIG. 5. Real part of dielectric constant (ϵ_1) of trigonal Se at 300°K.

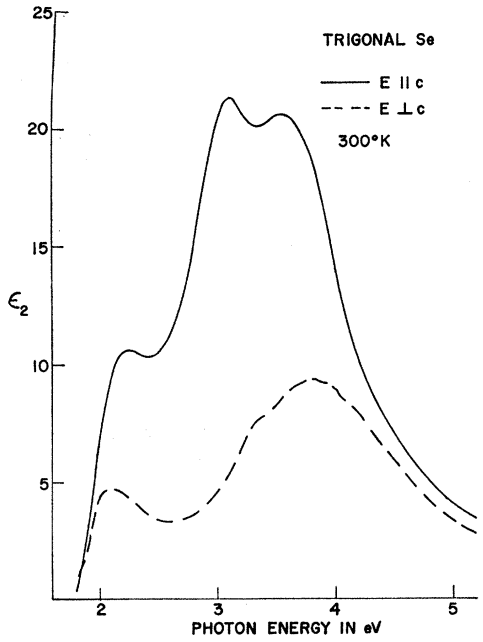

FIG. 6. Imaginary part of dielectric constant (ϵ_2) of trigonal Se at 300°K.

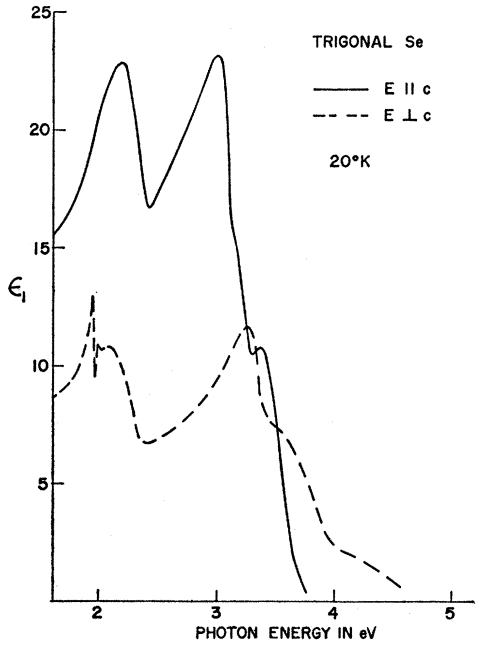

FIG. 7. Real part of dielectric constant (ϵ_1) of trigonal Se at 20°K.

[13] A. Smith, J. Opt. Soc. Am. 50, 862 (1960)

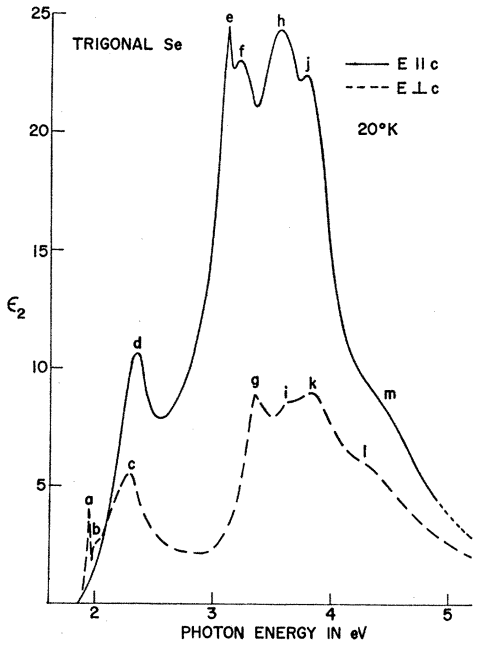

FIG. 8. Imaginary part of dielectric constant (ϵ_2) of trigonal Se at 20°K.

points were used to compute these constants for each mode of polarization at each temperature. From the values of ϵ_1 and ϵ_2 given in Figs. 5 to 8, the real and imaginary parts of the index of refraction, n and k, respectively, and the optical absorption coefficient α may be obtained by the following relations:

$$\epsilon_1 = n^2 - k^2,$$
$$\epsilon_2 = 2nk, \qquad (1)$$
$$\alpha = 4\pi k/\lambda,$$

where λ is the wavelength in cm.

The absorption spectra thus calculated are given in Fig. 9 for both modes of polarization at 20°K. The broken line shows the absorption spectrum for $E \perp c$ and the solid line the absorption spectrum for $E \| c$. In addition to the exciton absorption peak[11] found at 1.95 eV in the former curve, which takes place at the direct band edge, the peak at 3.10 eV in the latter curve is also interpreted as being caused by an exciton absorption. The absorption responsible for the latter exciton peak is interpreted as occurring at a saddle point Z in the Brillouin zone (Fig. 1). Portions of the absorption spectrum in the vicinity of these two exciton peaks are given in Fig. 10 to show their temperature dependence. The solid curves are for 20°K and the broken curves are for 300°K.

Since the imaginary part of the dielectric constant ϵ_2 is directly related to the density of states in the band-to-band one-electron transitions, the ϵ_2 spectrum at 20°K in Fig. 8 deserves the most attention. The structure observed is tabulated in Table I, which contains the peak positions in eV and their polarization dependence.

III. DISCUSSION

We have attempted without success to assign the observed peaks (Table I) to direct band-to-band transitions using the existing calculations.[5,7] Olechna and Knox[5] predicted that the band gap in a Se chain occurs at Z with both the conduction and valence bands being of Z_3 type. As elaborated in an earlier publication,[11] we have found that their assignment is not consistent with the observed polarizations of the first four peaks. On the other hand, the conduction and the valence bands at the minimum gap, as given by Sandrock and Treusch's calculation[7] for Se crystals, have the correct symmetries to explain the polarizations of the first four peaks[11] when spin-orbit coupling is taken into account. However, according to their band structure the next transitions should occur at Z between a Z_1 conduction band and a Z_3 valence band (in single-group representation). This would predict a transition with perpendicular polarization which is not observed.

Furthermore, modification of Sandrock and Treusch's model[7] by including spin-orbit coupling cannot account for the polarizations of the observed peaks e and f (Table I). In this situation, the Z_3 valence band is split into a complex conjugate doublet Z_4 and Z_5 and a spin doublet Z_6 (in double-group representation). The transition from the former level to the conduction band ($Z_4, Z_5 \rightarrow Z_6$) is allowed for $E \perp c$. The transition from the latter level to the conduction band ($Z_6 \rightarrow Z_6$) is allowed for both $E \perp c$ and $E \| c$.

It appears that the experimental evidence presented here makes a reconsideration of the band structure of

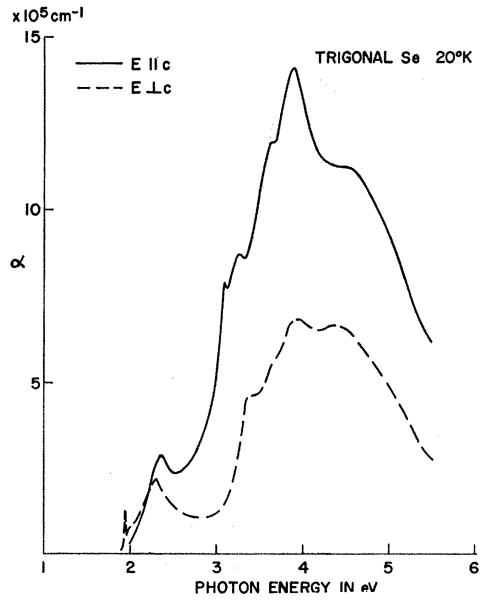

FIG. 9. Absorption coefficient α of trigonal Se at 20°K.

trigonal Se necessary. The following analysis differs from the previous ones[5,7] in its use of the molecular orbital method with suitably hybridized orbitals as basis functions.

In a helical chain of trigonal Se, the $4s$ and $4p$ atomic orbitals of each Se atom are hybridized into (1) two equivalent sigma orbitals pointing toward the nearest neighbors, and (2) two equivalent lone pair orbitals.[14] They can be written as

$$\begin{aligned}\sigma_1&=\gamma s+(1-\gamma^2)^{1/2}p_1,\\ \sigma_2&=\gamma s+(1-\gamma^2)^{1/2}p_2,\\ \lambda_3&=(0.5-\gamma^2)^{1/2}s+(0.5+\gamma^2)^{1/2}p_3,\\ \lambda_4&=(0.5-\gamma^2)^{1/2}s+(0.5+\gamma^2)^{1/2}p_4,\end{aligned}\tag{2}$$

where the coefficient γ can be determined from the bond angle[15] θ ($=103.1°$) as

$$\gamma=[-\cos\theta/(1-\cos\theta)]^{1/2}=0.43,\tag{3}$$

and the p functions are appropriate combinations of p_x, p_y, and p_z orbitals [Fig. 11(a)].

The sigma orbitals of two neighboring atoms A and B, pointing toward each other, form a bonding orbital β and an antibonding orbital α.

$$\begin{aligned}\beta&=[\sigma_1(A)+\sigma_2(B)]/[2(1+S_\sigma)]^{1/2},\\ \alpha&=[\sigma_1(A)-\sigma_2(B)]/[2(1-S_\sigma)]^{1/2},\end{aligned}\tag{4}$$

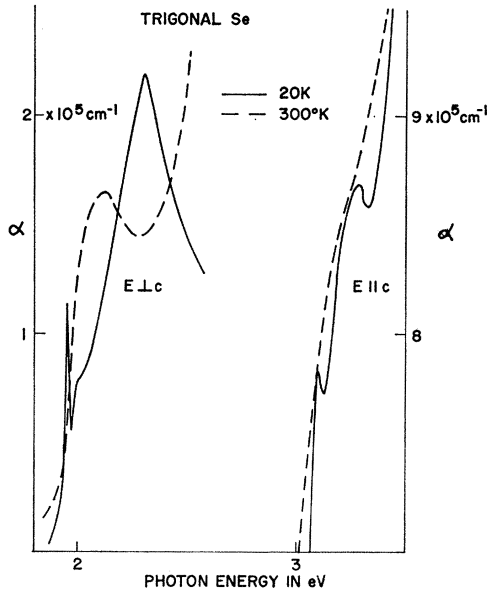

FIG. 10. Absorption coefficient α in the vicinities of the two exciton peaks at 300 and 20°K.

[14] I. Chen and T. P. Das, J. Chem. Phys. **45**, 3526 (1966); **45**, 3536 (1966).

[15] P. Cherin and P. Unger, in Proceedings of the 7th International Congress and Symposium of the International Union of Crystallographers, Moscow, 1966 (unpublished); Inorg. Chem. (to be published).

TABLE I. Energies of observed peaks and their polarizations.

Peak	Peak energy (eV)	Polarization
a	1.95[a]	⊥
b	2.01[b]	⊥
c	2.28	⊥
d	2.33	∥
e	3.09[a]	∥
f	3.19	∥
g	3.34	⊥
h	3.54	∥
i	3.62	⊥
j	3.76	∥
k	3.82	⊥
l	4.30	⊥
m	4.50	∥

[a] Exciton absorption peaks.
[b] The higher states ($n=2, 3, \cdots$) of the exciton (a) contribute to the shoulder of the peak (b).

where $S_\sigma=\langle\sigma_1(A)|\sigma_2(B)\rangle$ is the overlap integral between the two sigma orbitals.

The two lone pair orbitals λ_3 and λ_4 of the same atom can combine to form two new orbitals ρ and τ, which transform symmetrically and antisymmetrically, respectively, under a twofold rotation around an axis perpendicular to the c axis [Fig. 11(b)]. The orbital

$$\rho=(\lambda_3+\lambda_4)/\sqrt{2}\tag{5}$$

points radially outward from the cylindrical surface of the helix, and the orbital

$$\tau=(\lambda_3-\lambda_4)/\sqrt{2}\tag{6}$$

is a pure p orbital tangent to the same surface.

The sigma orbitals contribute to the covalent bonding in the chain and the ρ and τ orbitals are responsible for the weaker interchain forces.

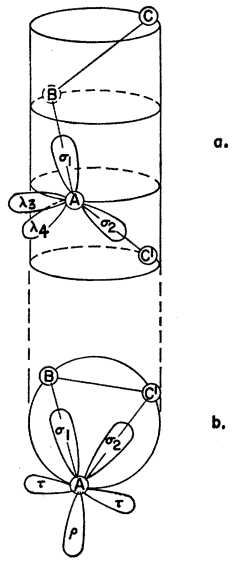

FIG. 11. Hybrid orbitals of Se in a helical chain.

The energies of these orbitals can be expressed in terms of E_s and E_p, the energies of $4s$ and $4p$ atomic orbitals in the valence state of Se, by

$$\begin{aligned} E_\rho &= (1-2\gamma^2)E_s + 2\gamma^2 E_\rho, \\ E_\tau &= E_p, \\ E_\alpha &= (E_\sigma - E_{\sigma\sigma'})/(1-S_\sigma), \\ E_\beta &= (E_\sigma + E_{\sigma\sigma'})/(1+S_\sigma), \end{aligned} \tag{7}$$

where $E_\sigma = \gamma^2 E_s + (1-\gamma^2)^{1/2} E_p$, and

$$E_{\sigma\sigma'} = \langle \sigma_1(A) | H | \sigma_2(B) \rangle.$$

Using the values[16] $E_s = -20.83$ eV and $E_p = -10.79$ eV, and the semiempirical formula[17]

$$E_{\sigma\sigma'} = S_\sigma(2 - |S_\sigma|)E_\sigma, \tag{8}$$

with $S_\sigma = 0.535$,[14] we obtain

$$\begin{aligned} E_\alpha &= -5.88 \text{ eV}, \\ E_\tau &= -10.79 \text{ eV}, \\ E_\beta &= -14.70 \text{ eV}, \\ E_\rho &= -17.12 \text{ eV}. \end{aligned} \tag{9}$$

Following Olechna and Knox,[5] we also consider the $5s$ atomic orbital in addition to the $4s$ and $4p$ atomic orbitals. The orbital energy of the former can be deduced from the atomic spectroscopic data[18] as $E_{5s} = -3.72$ eV.

Since there are six valence electrons per atom, the three lower-energy levels τ, β, and ρ are filled. These orbitals are the major constituents of the valence bands, with τ being the highest. The empty α and $5s$ orbitals constitute the major parts of the conduction bands.

Using the character tables of the groups of the wave vectors[19] we can classify the Bloch sums of each type of orbitals according to the irreducible representations of the group. Those for the Bloch sums at the four symmetry points Γ, K, Z, and H in the Brillouin zone (Fig. 1) are given in Table II.

With spin-orbit interaction, the doubly degenerate representations (Γ_3, K_3, Z_3, and H_3) are split into two levels. In the double-group representations, we have

$$\begin{aligned} &\Gamma_1 \rightarrow \Gamma_6, \\ &\Gamma_2 \rightarrow \Gamma_6, \\ &\Gamma_3 \rightarrow \Gamma_4, \Gamma_5, \Gamma_6, \end{aligned} \tag{10}$$

where Γ_4 and Γ_5 are complex-conjugate to each other, and Γ_6 is a spin doublet. The same relations hold for the representations at the other three points K, Z, and H.

The selection rules for dipole transitions are given in Table III. The $\perp$ and $\parallel$ signs refer to transitions which can be excited by light polarized perpendicular and parallel, respectively, to the c axis, and F denotes a forbidden transition.

Using the experimental information (the peak positions and their polarizations) and theoretical information (the symmetries of the conduction and the valence bands, and the selection rules), we have assigned the observed peaks in the ϵ_2 spectra (Fig. 8 and Table I) to direct band-to-band transitions as shown in Fig. 12. We have assumed that the singularities of ϵ_2 take place at the symmetry points Γ, Z, H, and K of the Brillouin zone. We also assumed that the band-gap energies at these points increase in the order H, Z, Γ, and K, as given by Sandrock and Treusch's calculation.[7]

It can be seen from Table II and relation (10) that, in the double-group representation, the conduction and the valence bands at the four symmetry points all contain the same types of species, namely, one set of complex-conjugate doublets (Γ_4, Γ_5, etc.) and two spin doublets (Γ_6, etc.). Thus the second assumption is only for the convenience of nomenclature. At each symmetry point there are nine different ways that the three species of the conduction band and the three species of the valence band can be ordered. Only one among them gives the correct sequence of the observed polarization. From our data, only the relative distances between the valence and conduction bands at the symmetry point can be determined. The relative positions between levels at different symmetry points cannot be fixed.

The first exciton peak a (at 1.95 eV: see Fig. 8) is associated with the direct band-gap transition at H, and the second exciton peak e (at 3.09 eV) is associated with the band edge transition at Z. The former has a half-width of 0.04 eV and a maximum absorption coefficient of 1.15×10^5 cm^{-1} at 20°K (Fig. 10). Applying the gen-

TABLE II. Irreducible representations of the Bloch sums of α-, τ-, β-, and ρ-type orbitals at the symmetry points Γ, K, Z, and H.

Symmetry point	$5s$	α Conduction band	τ Valence band	β	ρ
Γ	Γ_1,Γ_3	Γ_2,Γ_3	Γ_2,Γ_3	Γ_1,Γ_3	Γ_1,Γ_3
K	K_1,K_3	K_2,K_3	K_2,K_3	K_1,K_3	K_1,K_3
Z	Z_1,Z_3	Z_1,Z_3	Z_2,Z_3	Z_2,Z_3	Z_1,Z_3
H	H_1,H_3	H_1,H_3	H_2,H_3	H_2,H_3	H_1,H_3

TABLE III. Selection rules in double-group Γ of D_3^6. The same rules hold for K, Z, and H.

	Γ_4	Γ_5	Γ_6
Γ_4	F	$\parallel$	$\perp$
Γ_5	$\parallel$	F	$\perp$
Γ_6	$\perp$	$\perp$	$\parallel,\perp$

[16] C. J. Ballhausen and H. B. Gray, *Molecular Orbital Theory* (W. A. Benjamin, Inc., New York, 1964), p. 122.
[17] L. C. Cusachs, J. Chem. Phys. 43, S157 (1965).
[18] C. E. Moore, *Atomic Energy Levels*, Natl. Bur. Std. (U. S.) Circ. No. 467 (U. S. Government Publishing and Printing Office, Washington, D. C., 1949).
[19] M. Hulin, Ann. Phys. (Paris) 8, 647 (1963).

eralized Smakula equation[20] without any local-field correction, we find the oscillator strength for this transition to be 1.5×10^{-4}. This value is an order of magnitude smaller than the oscillator strength found for the first exciton peak in ZnO (13×10^{-4}) as reported by Thomas.[21] This accounts for the fact that the exciton peak in Se is not observed at 300°K, whereas the exciton peaks in ZnO are observable at 300°K.

The binding energy E_B of an exciton, in the effective-mass approximation for a uniaxial crystal, is given by

$$E_B=e^4\mu_0 m_0/2\hbar^2\epsilon_0^2 n^2=13.6\mu_0/\epsilon_0^2 n^2, \qquad (11)$$

where m_0 is the free-electron mass and n is an integer. The mean reduced mass μ_0 and the mean dielectric constant ϵ_0 are given by Hopfield and Thomas[22] as

$$\frac{1}{\mu_0}=\frac{2}{3}\frac{1}{\mu_\perp}+\frac{1}{3}\frac{1}{\mu_\parallel}\frac{\epsilon_\perp}{\epsilon_\parallel}, \qquad (12)$$

and

$$\epsilon_0=(\epsilon_\perp\epsilon_\parallel)^{1/2}, \qquad (13)$$

where $\mu_\perp$ ($\mu_\parallel$) is the reduced effective mass perpendicular (parallel) to the c axis in units of m_0, and $\epsilon_\perp$ ($\epsilon_\parallel$) is the dielectric constant perpendicular (parallel) to the c axis.

For the exciton a, $n=1$ and $E_B=0.06$ eV.[23] This binding energy is greater than any phonon energies observed,[24] which implies that the square of the refractive index measured near the exciton binding energy may be taken as the dielectric constant. From the refractive indices measured by Gobrecht and Tausend[10] (at room temperature), the values $\epsilon_\perp=8$ and $\epsilon_\parallel=13.3$ are obtained. Using these values, we find $\mu_0=0.47$ for the exciton a.

The exciton Bohr radius is given by

$$r=\hbar^2\epsilon_0/\mu_0 m_0 e^2=5.3\times10^{-9}(\epsilon_0/\mu_0)\text{ cm}. \qquad (14)$$

Using the value of μ_0 obtained above, we calculate $r=11.6$ Å. This value is sufficiently small to justify the use of the optical dielectric constant in the calculations above.[25]

Stuke and Weiser[26] observed the Franz-Keldysh effect in trigonal Se. From their measurements with light polarized perpendicular to the c axis, they calculated the reduced effective masses $\mu_\perp=1.47$ and $\mu_\parallel=0.22$. Substituting these values in Eq. (12) we obtain a value for the mean reduced mass $\mu_0=0.73$. This value is in fair agreement with the value calculated from the exciton binding energy above. Gobrecht and Tausend[27] deduced the effective mass of holes in trigonal Se from Faraday rotation measurements to be $m_h^*=2.7m_0$ at 2 eV for $E\perp c$. Using this value and $\mu_0=0.47$ obtained above, we estimate the effective electron mass to be about $0.6m_0$. It is interesting to note that the electron effective mass deduced from these measurements is two orders of magnitude less than that conjectured by Gobrecht and Tausend.[27]

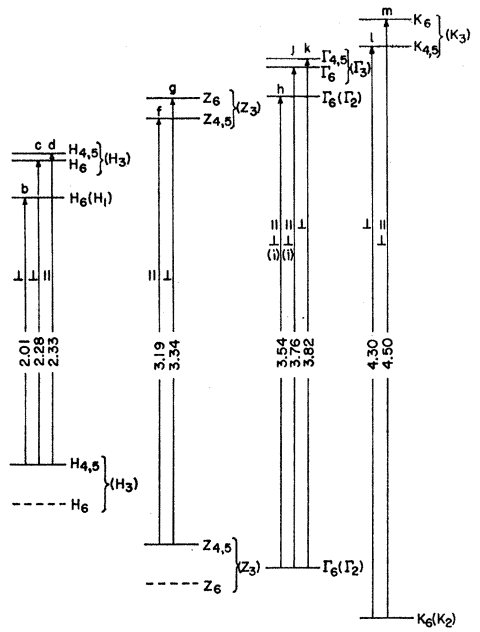

FIG. 12. Direct allowed transitions (in eV) in a proposed band scheme for trigonal Se at symmetry points H, Z, Γ, and K.

Because of the difficulty in determining the position of the onset of the transition f, the binding energy of the exciton e can only be estimated to be 0.07 ± 0.03 eV. This gives $\mu_0=0.55\pm0.23$ at the point Z in the Brillouin zone.

The spin-orbit splittings in the conduction band are 0.15 eV at Z and 0.20 eV at K, whereas that of atomic Se is 0.30 eV.[28] This shows that considerable amounts of $4s$ and $5s$ orbitals have mixed into the conduction band whose major constituents are the α-type orbitals. The mixing of $4s$ orbitals takes place through the hybridization to form sigma orbitals, and the $5s$ orbitals mix with the α orbitals because they form Bloch sums of the same irreducible representation (Table II). The spin-orbit splittings at H and Γ are further reduced (0.06 eV) by the nearby H_6 (H_1) and Γ_6 (Γ_2) levels. In the valence band where the major constituent is the τ orbital which is of pure p character, we expect the spin-orbit splitting

[20] D. L. Dexter, Phys. Rev. **101**, 48 (1956).
[21] D. G. Thomas, J. Phys. Chem. Solids **15**, 86 (1960).
[22] J. J. Hopfield and D. G. Thomas, Phys. Rev. **122**, 35 (1961).
[23] The value of the binding energy of the exciton a given in Ref. 11 (0.045 eV) has been revised after the completion of the Kramers-Kronig analysis of the reflectivity data.
[24] G. Lucovsky and R. C. Keezer, Bull. Am. Phys. Soc. **11**, 812 (1966); A. Mooradian and G. B. Wright, *ibid.* **11**, 812 (1966).
[25] R. S. Knox, *Theory of Excitons* (Academic Press Inc., New York, 1963), Sec. 4b.
[26] J. Stuke and G. Weiser, Phys. Status Solidi **17**, 343 (1966).
[27] H. Gobrecht and A. Tausend, in *Proceedings of the International Conference on the Physics of Semiconductors, Paris, 1964* (Academic Press Inc., New York, 1965), p. 1189.
[28] R. S. Knox, Xerox Research and Engineering Division Laboratories Report No. RL63-59 (unpublished); also see Ref. 14.

to be almost the same as that in atomic Se, as shown by the dotted lines in Fig. 12.

If the s orbitals were included in Sandrock and Treusch's calculation,[7] we would expect better agreement with the present experimental results. For example, according to their calculation the energy separation between the H_1 and H_3 conduction bands is about the same as the bandgap. Our results show that it is about 0.27 eV which is only one-seventh of the bandgap energy. If the $5s$ band were included in the calculation, the interaction between the bands could lower the H_3 band.

According to the assignments in Fig. 12, there should be two peaks at 3.54 and at 3.76 eV in the $E \perp c$ curve in Fig. 8. We observe only one broad peak at 3.62 eV (peak i). One might well be able to resolve fine structure in this peak by use of a modulated-reflectivity technique.

ACKNOWLEDGMENTS

During the course of this investigation we have profited greatly from discussions with many colleagures. In particular, we thank R. S. Knox and G. Lucovsky for their helpful comments. We are indebted to R. C. Keezer for supplying the sample crystals and to D. J. Olechna for the use of her computer program to calculate the Kramers-Kronig integrals. We are also indebted to A. Smith for the use of his vacuum uv monochromator. Thanks are also due to G. A. Charnitski and R. Walder for their assistance with the experimental work.

PHYSICAL REVIEW VOLUME 158, NUMBER 3 15 JUNE 1967

Measurements of the Thermal Conductivity of Single Crystals of Potassium between 2.5 and 40°K*

RONALD F. STAUDER†
The Catholic University of America, Washington, D. C.
AND
EUGENIE V. MIELCZAREK
The George Mason College of the University of Virginia, Fairfax, Virginia
(Received 26 August 1966; revised manuscript received 21 February 1967)

The thermal conductivity of two single crystals of potassium (ZK-1, ZK-2) was measured from 2.5° to 40°K. Measurements on a third crystal were made between 10° and 40°K. Additional measurements at 77°K were made on all three crystals. The results are in agreement with the previous measurements of MacDonald, White, and Woods with the exception that the two crystals whose measurements were carried through the conductivity maximum (ZK-1 and ZK-2) exhibited a higher conductivity at the maximum than can be accounted for by electronic conduction. This additional conductivity can be attributed to heat conduction by transverse phonons which, because of the sphericity of the potassium Fermi surface, are not interacting with the free electrons.

I. INTRODUCTION

THE alkali metals, particularly potassium, have been the subject of many recent theoretical and experimental investigations.[1–9] However the difficulties inherent in the handling of these soft reactive metals have curtailed measurements of their transport properties. The most recent measurements of this type were the measurements of the thermal and electrical conductivities of lithium, sodium, potassium, rubidium, and cesium samples which were encapsulated in glass tubes.[1] With the development of techniques for the growing of single crystals of sodium and potassium,[7,9] it became feasible to attempt transport measurements in single crystals of potassium. This paper is concerned with measurements of the thermal conductivity of three single crystal samples of potassium from 2 to 40° K. The first section of the paper gives a description of those facets of the experimental techniques which pertain particularly to the special problems encountered in making a thermal conductivity measurement on an alkali metal. The second section gives a brief summary

* The experimental work was performed at the Catholic University of America under U. S. Atomic Energy Commission Contract No. AT(40-1)-2861.

† Present address the Johns Hopkins Applied Physics Laboratory, Silver Springs, Maryland. This work was submitted in partial fulfillment to the Catholic University of America for the requirements for the degree of Doctor of Philosophy.

[1] D. K. C. MacDonald, G. K. White, and S. B. Woods, Proc. Roy. Soc. (London) **A235**, 358 (1956).
[2] J. Filby, and D. Martin, Proc. Roy. Soc. (London) **A284**, 83 (1965).
[3] C. Monfort and C. Swenson, J. Phys. Chem. Solids **26**, 291 (1965).
[4] D. Schoenberg and P. Stiles, Proc. Roy. Soc. (London) **281**, 62 (1964).
[5] C. Grimes and A. Kip, Phys. Rev. **132**, 1991 (1963).
[6] H. Foster, P. Meijer, and E. Mielczarek, Phys. Rev. **139**, 1849 (1965).
[7] F. Hoyt and E. Mielczarek, Appl. Mat. Res. **4**, 121 (1965).
[8] W. B. Marquardt and J. Trivisonno, J. Phys. Chem. Solids **26**, 273 (1965).
[9] W. B. Daniels, Phys. Rev. **119**, 1246 (1960).